Crystallography of Hydrides in Textured Zircaloy-4 Sheets

N.A.P.Kiran Kumar[1], Jerzy.A. Szpunar[1] and Zhang He[2]
[1] McGill University, Quebec, Canada
[2] Atomic Energy of Canada Limited,
Chalk River Laboratories, Ontario, Canada

Abstract

Cold-worked and stress-relieved (CWSR) Zircaloy-4 sheet-samples were charged with 45 to 247 ppm of hydrogen using an electrolytic technique. Optical microscopy shows stacks of hydride platelets oriented along the rolling direction of the samples. Morphology and orientation of the hydrides was examined using the Electron Backscatter Diffraction (EBSD) technique. The hydrides, identified as $\delta_{ZrH1.5}$ phase by the EBSD analysis, were located both within the grains and along the grain boundaries, but the grain boundary hydrides appeared to be dominant. The hydrides and the matrix have the $(0001)_{\alpha\text{-}Zr}//(111)\delta_{ZrH1.5}$ orientation relationship at all locations. Also, the hydrides show strong {111} texture with maxima located at the same angle on the pole figure as the maxima of basal plane of the α-zirconium matrix. The reproducibility of the results was verified using samples with different hydride concentrations.

1. Introduction

Zircaloy-4 is widely used as a key structural material (e.g., cladding material) of [1]CANDU® fuel-bundles. Hydrogen pick-up during fuel-bundle irradiation leads to formation of hydrides, often in the form of platelets in the material. These hydrides have a deleterious impact on the mechanical properties of the material. Thus, an in-depth understanding of the hydriding process and the hydride orientation relative to the α-zirconium matrix should contribute to improvement in fuel-manufacturing technologies and may increase fuel safety margins.

It is well known that the hydrogen solubility in the α-Zirconium matrix decreases rapidly from 6 at% at 550°C, to 0.7 at% at 300°C, and 10^{-4} at% at room temperature [1] and that excess hydrogen is precipitated from the matrix in the form of zirconium hydrides. Three stoichiometric hydride phases were reported earlier and which one is formed depends on the cooling rate and hydrogen concentration. Among the hydrides, γ–hydride (FCT) is a metastable phase formed on fast cooling, δ-hydride (FCC) is considered to be a stable phase that is formed during slow cooling and ε-hydride (FCT) is formed at higher hydrogen concentration (63 at%) [2]. It is well known that the δ-hydride phase is most often formed in the material during bundle irradiation; however, formation mechanisms of the δ-hydrides [3, 4], including the nucleation and growth processes, need to be further examined.

It has been proposed that, in unstressed samples, hydrides would grow into grains along particular habit planes of the matrix [5, 6]. Various habit planes have been suggested to date, like the prism plane {10-10}, pyramidal plane {10-11}, basal plane (0001), {10-17} and twinning planes {10-12}, {11-21} and {11-22} of the HCP matrix. Insufficient evidence has been presented to support these assignments however, and the fact that many habit planes have been suggested makes it difficult to understand the crystallographic relationship between the hydrides

[1]CANDU® is a registered trademark of Atomic Energy of Canada Limited (AECL).

and the matrix. A few researchers reported that the hydride preferential sites are grain boundaries (inter-granular hydrides) but could not come up with rationalized notations [7]. A few papers reported the crystallographic relation of the inter-granular hydrides in Zircaloy-2 [3, 6, 9, and 10]. Zircaloy-4, which has slightly higher iron content and almost no nickel, shows better resistance to hydrogen pickup than Zircaloy-2 [11]. However, the amount of hydrogen pick up in the material increases with fuel irradiation time; and therefore, a thorough understanding of hydride precipitation behavior in Zircaloy-4 is needed for further improvement of fuel irradiation performance.

The objective of the present investigation was to determine the crystallographic relationship between δ-hydrides and the matrix in Zircaloy-4 CWSR sheet using EBSD. Because Zircaloy-4 sheet- and tubing-materials are both used for fabrication of CANDU fuel bundles, and they have very similar texture and hydrogen pick-up behavior, the results of this investigation are also applicable to the tubing material.

2. Experimental

The chemical composition of the Zircaloy-4 sheet-material is given in Table 1. The samples, provided by Atomic Energy of Canada Limited (AECL), were elecrolytically hydrided in a 0.125 molar H_2SO_4 solution at AECL Chalk River Laboratories. Hydrogen content in the samples was varied from 45 ppm to 247 ppm by controlling the electrolysis time. After the charging, the samples were homogenized by heating them at 375°C for 3 hours and then furnace cooled to room temperature to obtain a homogeneous distribution of hydrides.

Table 1: Alloy composition of Zircaloy-4

	Sn (wt%)	**Fe** (wt%)	**Cr** (wt%)	**Ni** (wt%)	**Nb** (wt%)	**O** (wt%)	**Zr** (wt%)
Zircaloy-4	**1.52**	**0.21**	**0.11**	**<35 ppm**	**-**	**0.125**	**bal**

The samples for EBSD analysis were prepared by etching them in solutions of 45% HNO_3, 45% H_2O and 10% HF, followed by colloidal silica polishing. The EBSD measurements were carried out with an Orientation Imaging Microscopy (OIM) system, installed on a FEG XL30 scanning electron microscope (SEM). The EBSD patterns were obtained and analyzed by means of the TSL OIM software.

2.1 The Reference Frame for Electron Backscatter Pattern (EBSP) Analysis

The Zircaloy-4 sheet directions represented in the present optical, EBSD and texture analyses are RD, TD and ND as show in Figure 1, where RD is the rolling direction of the sheet, TD is the transverse direction and ND is the normal direction.

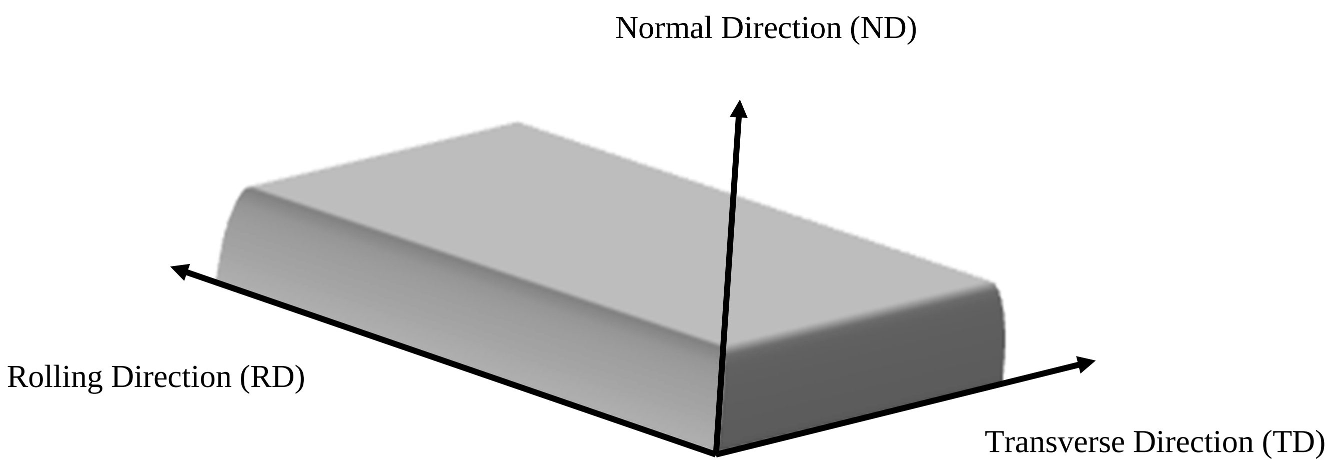

Figure 1: Directions of the Zircaloy-4 sheet samples.

3. Results

3.1 Optical Microscopy

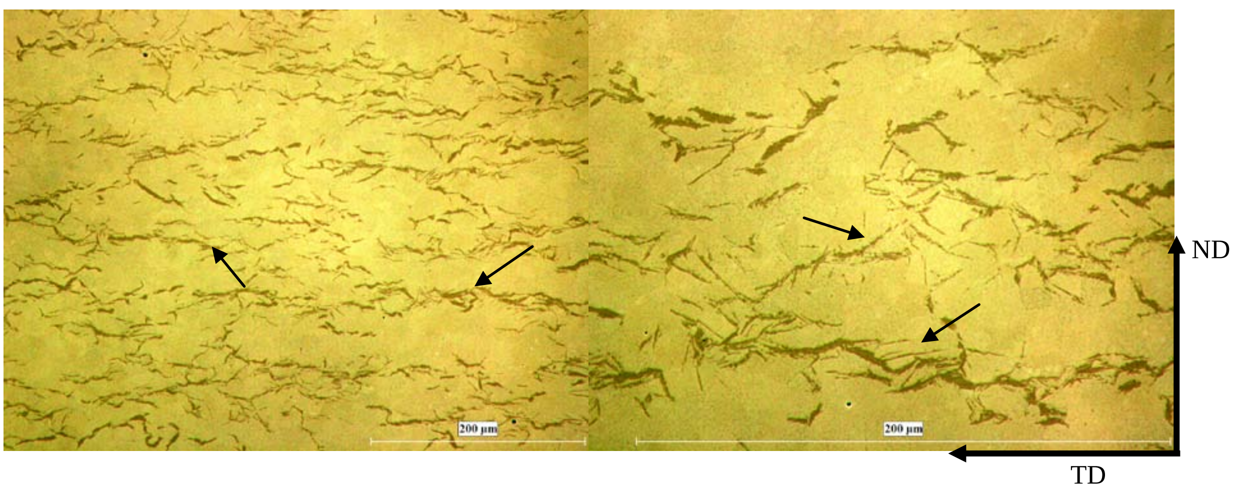

Figure 2: Typical optical micrographs of the sample with ~247 ppm of hydrogen. Note the hydrides (arrow) are along the TD direction.

Optical examination of the hydrided samples revealed that the hydrides were distributed along the transverse direction (TD) of the samples (see Figure 2 as an example). The grain boundaries are however not discernable optically, and thus, we cannot obtain any detailed information regarding location of the hydrides with respect to the grains and grain boundaries. However, this information is crucial for understanding the mechanical behavior of the material, for example, fracture mechanism of it under load.

3.2 Hydride Crystallographic Orientation

The EBSD technique can not only identify hydride phases by indexing their characteristic diffraction patterns but also determine their crystallographic orientations with respect to Zircaloy-4 grains and grain boundaries. Kikuchi patterns indexed with EBSD system show the presence of the α–Zirconium (HCP) matrix and δ-hydrides (FCC), with some negligible amount of γ -hydride, which is considered to be stable only at high cooling rates [2]. Figure 3 shows a grain map of a hydrided sample where each grain is mapped with different color code based on the crystal orientation. As shown, the matrix has the characteristic CWSR microstructure characterized by the presence of elongated grains along the rolling direction (RD). For better contrast, the hydrides are marked with red color.

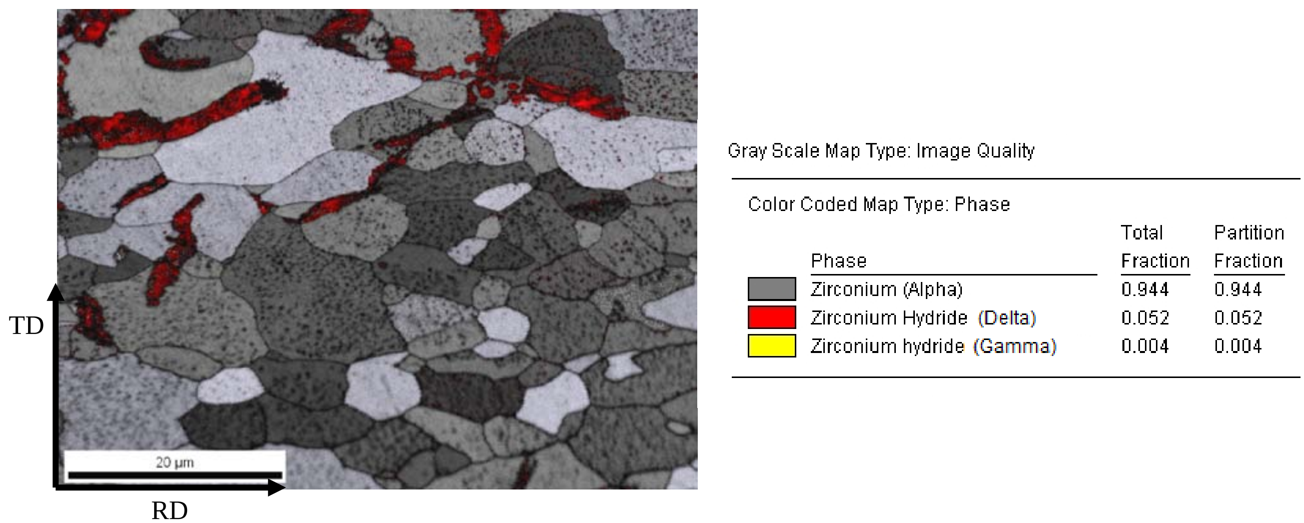

Figure 3: EBSD grain map of Hydrided Zircaloy-4 samples.

The α-Zirconium (HCP) matrix and δ-Zr-$H_{1.5}$ (FCC) hydrides are indentified using the standard Kikuchi pattern of Zirconium (JCPDS 00-005-0665) and Zirconium Hydride (JCPDS- 00-008-0218), respectively. As shown in Figure 3, the hydride precipitation took place both inside the grains and along the grain boundaries. EBSD was also recorded at lower magnification as shown in Figure 4, in order to obtain good statistical data about the hydride precipitation sites.

Out of 150 analyzed locations 97 were observed to be grain-boundary hydrides, where as 53 were intra-granular (within the grains) hydrides. So the ratio of intra-granular hydrides to inter-granular hydrides is about 1.8, which suggests that hydride precipitation along the grain boundaries is predominant.

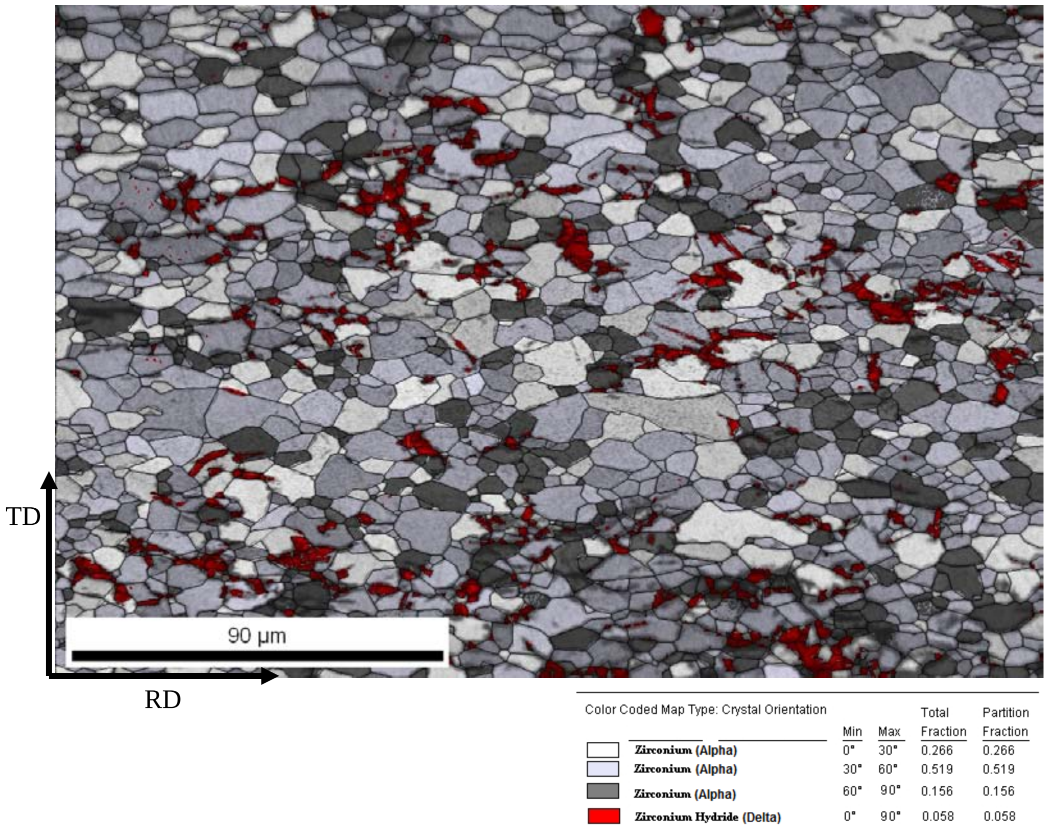

Figure 4: EBSD grain map of hydrided sample at lower magnification

3.2.1 Intra- and Inter-granular hydrides

In the literature [14, 15] different habit planes were suggested for intra-granular hydrides. To determine the habit plane for the present samples, the crystallographic relationship between the hydrides and the α-Zirconium matrix was analyzed using the pole figure method. The hydrides were observed within the grains, although they are in contact with the grain boundaries along its length. At all points the intra- and inter-granular hydrides were found to be following the $(0001)_{\alpha\text{-}Zr}//(111)\delta_{ZrH1.5}$ relationship as illustrated in Figure 5.

A closer look at some grain boundary hydrides (e.g., point (h) in Figure 5) shows that the hydrides are clustered near the grain boundaries but not exactly at the grain boundaries. They are very close to the grain boundaries; however, the necessary requirement of the $(0001)_{\alpha\text{-}Zr}//(111)\delta_{ZrH1.5}$ orientation relationship is clearly met.

The hydride precipitation is reported to be associated with micro stresses which arise from cold working [13]. But this is ruled out in the present case as the sample is stress relieved. Perhaps the most revealing part of the presented analysis is that, irrespective of hydride location, the hydrides all follow the $(0001)_{\alpha\text{-}Zr}//(111)\delta_{ZrH1.5}$ orientation relationship with the α-Zirconium matrix.

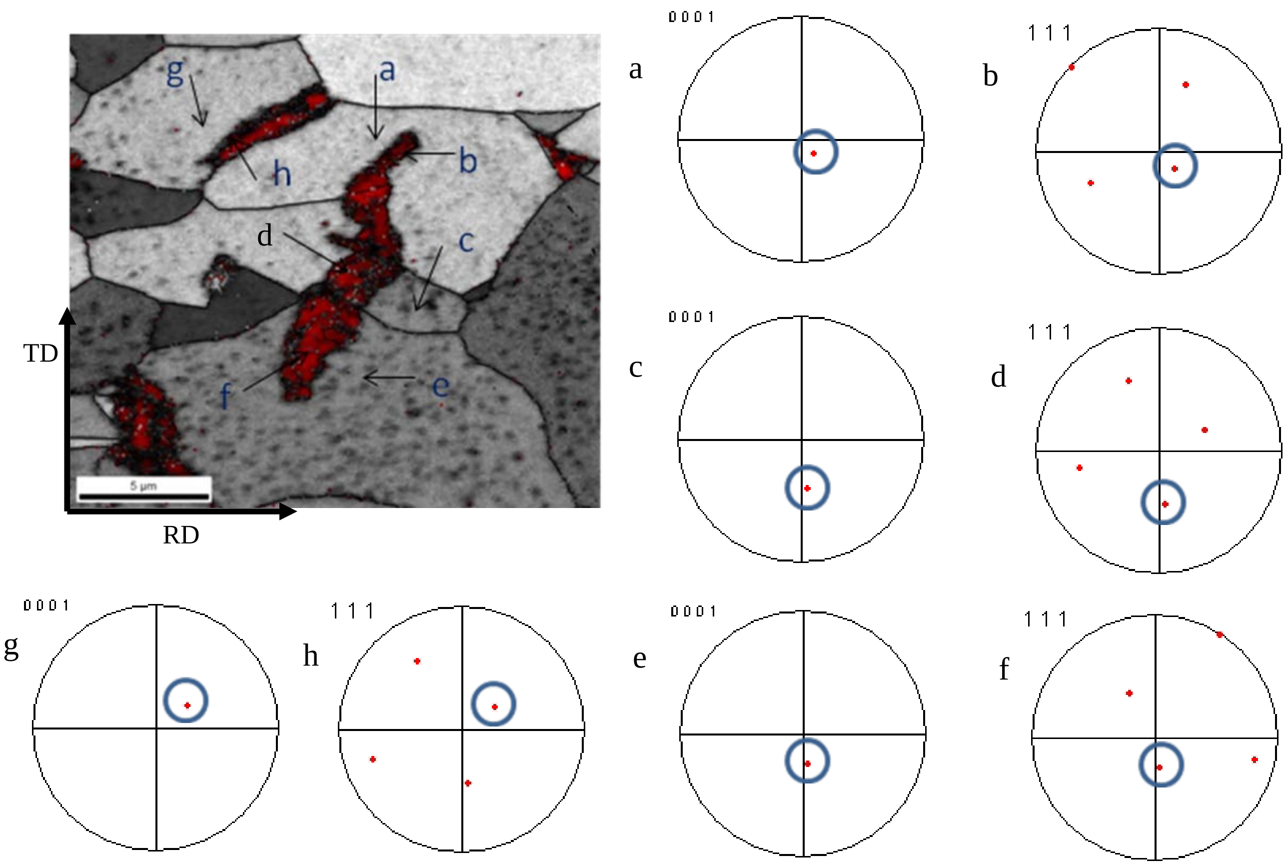

Figure 5: Zirconium hydrides precipitated within grains and at grain boundaries

3.3 Sample with low hydrogen concentration

Experiments were performed on the sample with 117 ppm of hydrogen in it. Figure 6 shows a typical EBSD pattern of the sample. A lower number of small hydrides is recorded however even in this case the hydrides still followed the $(0001)_{\alpha\text{-Zr}}//(111)\delta_{ZrH1.5}$ orientation relation, irrespective of the hydride location.

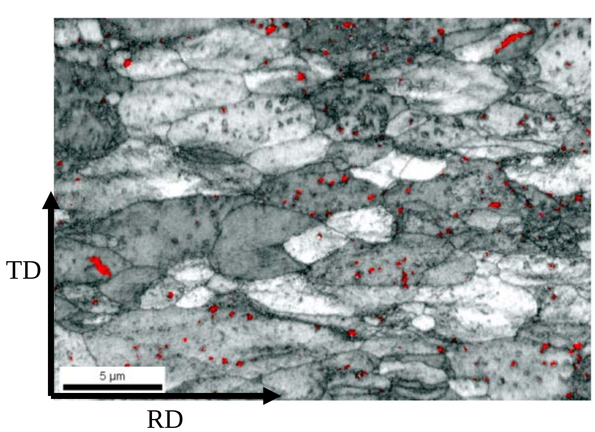

Figure 6: EBSD gain map of sample with 117 ppm hydrogen concentration.

3.4 Texture

The macro and micro texture data were obtained from X-ray diffraction (XRD) and EBSD techniques, respectively. Both show strong (0002) basal plane texture, a typical texture of CWSR Zircaloy-4 material, as shown in Figure 7.

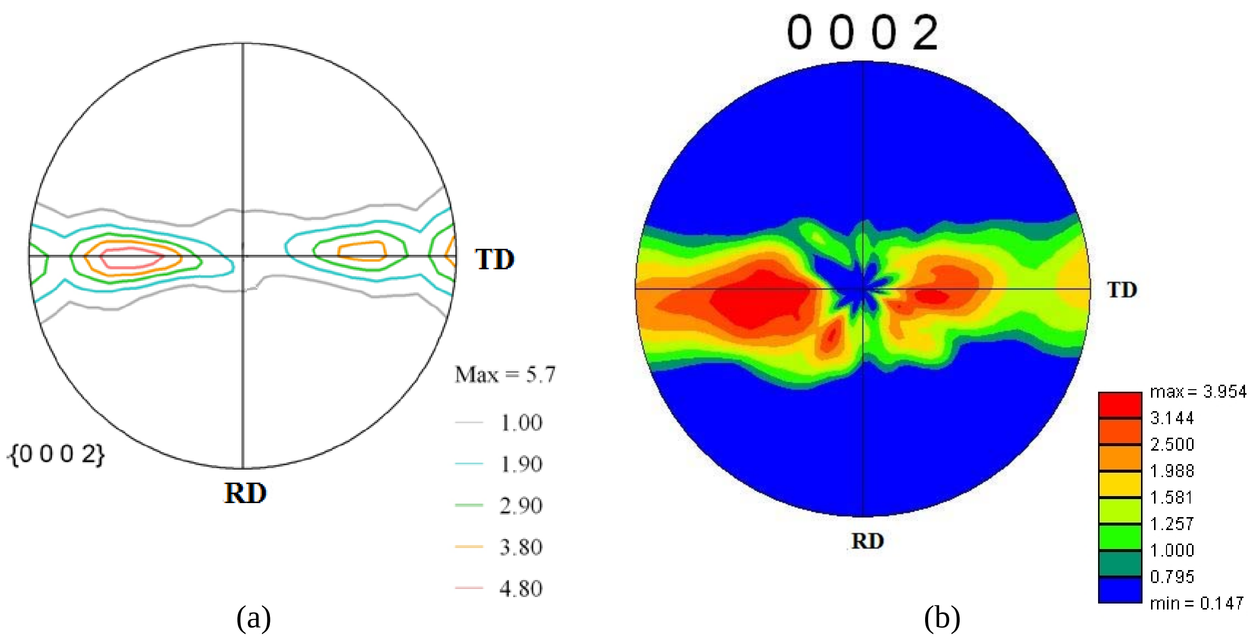

Figure 7: (0002) basal plane texture of CWSR Zircaloy-4 sheet, a) macro texture determined by XRD and b) micro texture determined by EBSD.

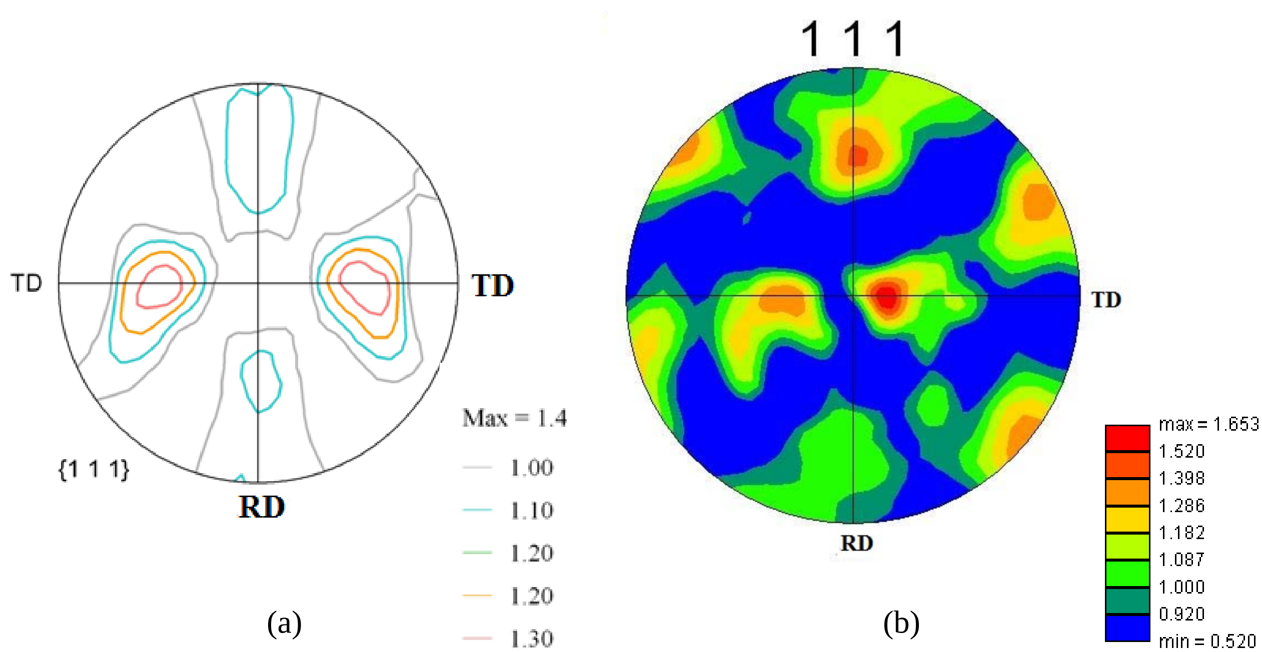

Figure 8: Texture of Zirconium hydride (δ-ZrH1.5), a) macro texture, and b) micro texture.

Interestingly, both the micro and macro texture analyses of the hydride phase show that the zirconium hydride has a strong {111} texture and if we compare the results presented in the pole figures of Figures 7 and 8, we can find that, the peak of the basal plane of Zirconium and the {111} plane of zirconium hydride are at the same location (i.e., the areas color-coded in red in the pole figures). That implies that {111} plane of zirconium hydrides always prefer to orient parallel to the (0002) basal plane of the matrix.

The present study documents the orientation relationship between the hydrides and the zirconium matrix in CWSR Zircaloy-4 samples. It supports the interpretation of hydride formation proposed by K. Une et al [12] for Zircaloy-2 samples.

4. Conclusions

The crystallographic orientation between the hydrides and a CWSR Zircaloy-4 matrix was examined using the EBSD technique. The following conclusions can be derived based on the results of this investigation:

1. Statistical data on hydrided sample (247 ppm) shows that the ratio of number of inter-granular to intra-granular hydrides is about 1.8 in CWSR Zircaloy-4 sheet.
2. Both inter-granular and intra-granular hydrides are found to follow the $(0001)_{\alpha\text{-}Zr}//(111)\delta_{ZrH1.5}$ orientation relationship with the zirconium matrix.
3. The hydrides show strong {111} texture with maxima located at the same angle on the pole figure as the maxima of the basal plane of zirconium.
4. A decrease in hydrogen concentration has no effect on the $(0001)_{\alpha\text{-}Zr}//(111)\delta_{ZrH1.5}$ orientation relationship.

5. References

[1] J.J. Kearns, “Terminal solubility and partitioning of hydrogen in the alpha phase of zirconium, Zircaloy-2 and Zircaloy-4”, Journal of Nuclear Materials, Vol. 22, Iss. 3, (1967), pp 292-303.

[2] D.O. Northwood and U. Kosasih, “Hydrides and delayed hydrogen cracking in zirconium and its alloys”, International Metals Reviews, Vol. 28, Iss. 2, (1983), pp 92-121

[3] M.P. Cassidy and C.M. Wayman, “The crystallography of hydride formation in zirconium: I.δ-γ transformation”, Metallurgical and Materials Transactions A, Vol. 11, Iss. 1, (1980), pp 47-56.

[4] S.S. Sidhu, N.S. Satya Murthy, “Neutron and X-ray diffraction studies of nonstoichiometric metal hydrides”, Advances in Chemistry, Vol. 39, (1963), pp 87-98.

[5] V.S. Arunachalam, B. Lehtinen and G. Ostberg, “The orientation of zirconium hydride on grain boundaries in Zircaloy-2”, Journal of Nuclear Materials, Vol. 21, Iss. 3, (1967), pp 241-248.

[6] D.G. Westlake, “The habit planes of zirconium in zirconium and Zircaloy”, Journal of Nuclear Materials, Vol. 26, Iss. 2, (1968), pp 208-216.

[7] K.V. Mani Krishna, A. Sain, I. samajdar, “Resistance to hydride formation in zirconium: An emerging possibility”, Acta Materialia, 54, (2006), pp 4665-4675.

[8] K. Une and Kazuhiro Nogita, “Crystallography of zirconium hydrides in recrystallized Zircaloy-2 fuel cladding by electron backscatter diffraction”, Journal of Nuclear Science and Technology, Vol. 41, Iss.7, (2004), pp 731-740.

[9] J.S. Bradbrook, G.W. Lorimer and N. Ridley, “The precipitation of zirconium hydride in zirconium and Zircaloy-2”, Journal of Nuclear Materials, Vol. 42, Iss. 2, (1972), pp 142-160.

[10] D.G. Westlake, “Diposition of hydrogen in quenched zirconium-hydrogen alloys”, Journal of Nuclear Materials, Vol. 16, Iss. 2, (1965), pp 215-219.

[11] Philip A. Schweitzer, “Corrosion engineering hand book”, Marcel Dekker, Inc. July (1996).

[12] K. Une and S. Ishimoto, “EBSP measurements of hydrogenated Zircaloy-2 claddings with stress relieved and recrystallized annealing condition”, Journal of Nuclear Materials, Vol. 357, Iss.1-3, (2006), pp 147-155.

[13] R.P. Marshall, "Influence of fabrication history on stress-oriented hydrides in Zircaloy tubing", Journal of Nuclear Materials, Vol.24, Iss.1, (1967), pp 34-48.

[14] C.E. Ells, "Hydride precipitates in zirconium alloys (A review)", Journal of Nuclear Materials, Vol. 28, Iss. 2, (1968), pp 129-151.

[15] V. Perovic, G.C. Weatherly and C.J. Simpson, "Hydride precipitation in α/β zirconium alloys", Acta Metallurgica, Vol. 31, Iss. 9, (1983), pp 1381-1391.